

## Oxygen dynamics in the rhizosphere of *Zostera marina*: A two-dimensional planar optode study

Morten S. Frederiksen<sup>1</sup>

Institute of Biology, University of Southern Denmark, Campusvej 55, DK-5230 Odense M, Denmark

Ronnie N. Glud<sup>2</sup>

Marine Biological Laboratory, University of Copenhagen, Strandpromenaden 5, DK-3000 Helsingør, Denmark

### Abstract

The oxygen dynamics in the rhizosphere of *Zostera marina* was studied by use of planar optodes. Oxygen leakage to the rhizosphere was restricted to the root tip and extended only up to ~8 mm up along the root. The oxic sediment volume around the roots increased linearly with irradiance in the interval of 0–250  $\mu\text{mol photons m}^{-2} \text{ s}^{-1}$ , but the leakage rate saturated at the maximum irradiance of 500  $\mu\text{mol photons m}^{-2} \text{ s}^{-1}$ . Oxygen leakage decreased by ~60% from light to darkness and *Z. marina* was able to maintain an oxic zone around the root tip even in darkness as long as oxygen in the overlying water was at 100% air saturation (280  $\mu\text{mol L}^{-1}$ ).  $\text{O}_2$  leakage from the root tips stopped at 25% air saturation (70  $\mu\text{mol L}^{-1}$ ) and the oxic microniche rapidly disappeared. Increasing the oxygen concentration above 100% air saturation induced oxygen leakage from zones that otherwise appeared impermeable to oxygen. The roots on average grew by 8.7 mm  $\text{d}^{-1}$ , and a series of  $\text{O}_2$  images documented the high spatial and temporal dynamics of the oxic microniches around the root tips. The estimated total oxygen release to the rhizosphere of *Z. marina* beds was 2.3  $\text{mmol m}^{-2} \text{ d}^{-1}$ , which only corresponded to 12% of the diffusive oxygen uptake at the primary sediment–water interface. Rhizospheres of seagrass are thus probably of minor importance for total benthic  $\text{O}_2$  uptake rates.

Seagrasses are worldwide distributed and are estimated to cover ~10% of coastal sediments (Charpy-Roubaud and Sournia 1990). The plants colonize a wide range of sediment types, and their roots are, in most cases, growing in anoxic and highly reduced environments. Being obligate aerobes, seagrasses have adapted efficient strategies to maintain oxia in their root systems via an interconnected system of gas spaces (lacunae) transporting  $\text{O}_2$  from the leaves down to the roots (Penhale and Wetzel 1983; Larkum et al. 1989). The oxygen transport is driven by a partial-pressure gradient from the photosynthetically active leaves toward the  $\text{O}_2$ -consuming root system. However, radial oxygen loss (ROL) from the roots into the sediment may occur (Caffrey and Kemp 1991; Pedersen et al. 1998), and the oxygenated zones along roots have been suggested to be an adaptive feature providing an oxidative shield against harmful phytotoxins, such as  $\text{Fe}^{2+}$ ,  $\text{Mn}^{2+}$ , and sulfides (Penhale and Wetzel 1983). Recent studies of *Halophila ovalis* and *Zostera marina* have shown that a barrier against ROL exists along most of the root length (Connell et al. 1999; Jensen et al. 2005). The

barrier reduces ROL in the basal part of the root and increases the oxygen transport toward the actively growing root tip, consisting of cells with a high metabolic rate. Our present knowledge on the anatomical basis for the barriers against ROL in rooted macrophytes is very limited, but it is probably related to densely packed cells, suberin deposits, and lignification of the outer cell layers (Sorrel and Boon 1994; Barnabas 1996; Armstrong et al. 2000). Hence, oxygen leakage in seagrasses is confined to a relatively narrow region at the root apex (Connell et al. 1999; Jensen et al. 2005), creating a dynamic oxic sphere around the growing root tip.

Several techniques have been used to measure oxygen release from seagrass roots, but all have potential drawbacks compromising extrapolations to natural conditions (Sorrell and Armstrong 1994; Borum et al. in press). Split-chamber techniques where the roots are placed in an anoxic medium (or an oxygen-consuming medium) isolated from the overlying water have traditionally been used to measure total oxygen leakage from plant rhizospheres (Sand-Jensen et al. 1982; Caffrey and Kemp 1991). But typically, such systems poorly reflect natural conditions in marine sediments hosting a complex microbial community. Furthermore, split-chamber techniques provide a measure on whole-root oxygen excretion and provide little information on where and how  $\text{O}_2$  is leaving the complex root system. Some insight on these aspects has been provided by microelectrode studies offering detailed analysis of single roots and the option of studying the plants in a natural environment (Caffrey and Kemp 1991; Pedersen et al. 1998; Connell et al. 1999). This, however, can be an extremely tedious task of looking for the needle in the haystack and, thus, various manipulative procedures for microsensor studies have been developed (Pedersen et

<sup>1</sup> Present address: Greenland Institute of Natural Resources, Kivioq 2, Box 570, 3900 Nuuk, Greenland.

<sup>2</sup> Corresponding author (rnglud@bi.ku.dk).

### Acknowledgments

We thank A. Glud for construction of microelectrodes and manufacturing of planar optodes. J. Borum and two anonymous reviewers are thanked for constructive critique during the review process.

The study was financially supported by grants from the Danish Natural Science Research Council, the Carlsberg Foundation, and the EU Commission (contract numbers EVK3-CT2001-00210, EVK-CT2002-0076, GOCE-CT2003-505564, Q5RS-2001-02456). The support is gratefully acknowledged.

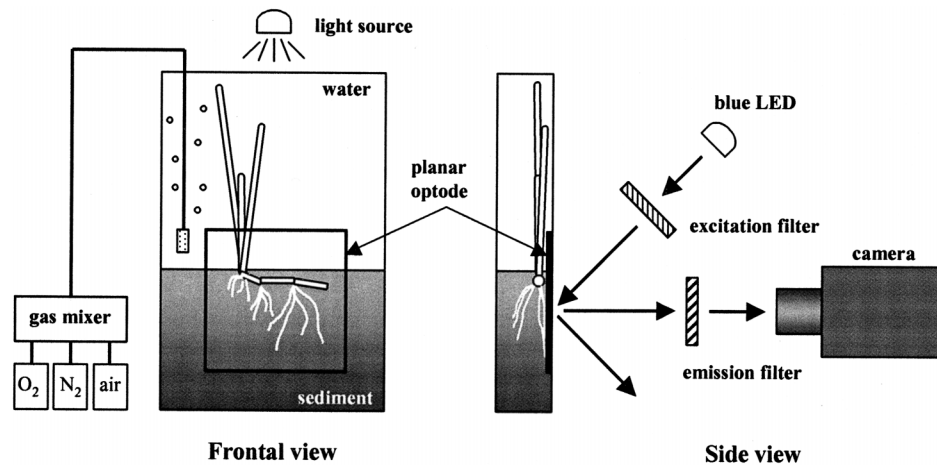


Fig. 1. Schematic drawing of the experimental setup (not to scale). The left side of figure shows a frontal view of the aquarium with the planar optode mounted between the sediment and the glass. The right side shows the aquarium from the side and the setup for light emission and camera recording. Arrows indicate the light paths of the excitation and emission light.

al. 1998; Jensen et al. 2005). These, to various extents, compromise the in situ interaction between the roots and the sediment. Moreover, the sensors, despite their excellent performance on small temporal and spatial scales, only resolve conditions at a selected spot of the root at a given time. Simultaneous measurements of temporal changes in  $O_2$  concentrations are possible but require a series of sensors, which, in most cases, is very impractical and compromised by root growth. Hence, microelectrode studies of rhizosphere oxygen dynamics in submerged plants have often been based on relatively few oxygen profiles that are extrapolated to the root level or even plant and community level (Pedersen et al. 1998; Holmer et al. 2002), which may lead to overgeneralized conclusions. To our knowledge, only two microelectrode studies have reflected the variations in ROL along seagrass root sections (Connell et al. 1999; Jensen et al. 2005), and only Jensen et al. (2005) had the roots placed in natural sediment. To map the  $O_2$  distribution around buried intact root systems as function of various environmental controls during active root growth by microelectrodes is extremely challenging. Recently, planar optodes have been introduced to benthic ecology providing two-dimensional images of  $O_2$  distribution in the sediment with high spatial ( $\sim 100 \mu\text{m}$ ) and temporal resolution (Glud et al. 1996). This technique has previously been used to study oxygen dynamics across various benthic water interfaces, (e.g., Precht et al. 2004; Wenzhöfer and Glud 2004), and very recently, the potential of planar optodes for rhizosphere studies have been presented (Jensen et al. 2005).

In this study, we use planar optodes to study oxygen dynamics in the rhizosphere of *Z. marina* and, for the first time, provide a detailed description of two-dimensional changes in oxygen distribution around roots under various light regimes, oxygen concentrations in the overlying water column, and as a function of root age. The oxygen leakage during rhizosphere development in natural sediment is directly monitored and the results are discussed quantitatively.

## Materials and methods

**Study site**—Plants of eelgrass (*Z. marina*) were collected at Svenstrup ( $55^{\circ}28.099'N$ ,  $9^{\circ}45.194'E$ ), Denmark, during October 2004 from a sandy-silt sediment at approximately 1 m of water depth. Plants were collected by digging out intact sediment blocks followed by gentle rinsing of the plant roots. The sediment was sieved through a 1-mm sieve and brought back to the laboratory together with the plants and 200 liters of seawater from the station (temperature  $12^{\circ}\text{C}$ , salinity of 21). In the laboratory, the plants were replanted in five aquaria containing the homogenized sediment overlain by the sampled seawater (Fig. 1). Each aquarium was equipped with a transparent planar optode (see following) fixed along one of the glass walls by a thin water film and tape along the edges. The plants were positioned close to but not in contact with the optode. The aquaria were placed in a large (100-liter) aerated storage aquaria and left for acclimation for a 3-week period at  $13^{\circ}\text{C}$  and a 12:12 light:dark (LD) cycle (irradiance  $\sim 250 \mu\text{mol photons m}^{-2}$ ). This period allowed new leaves and root bundles to develop, and roots gradually grew into the sediment along the planar optodes. During the acclimation phase, the sides of the aquaria were covered by black plastic to avoid development of microphytes along the aquaria walls. The subsequent planar  $O_2$  measurements were thus performed on undisturbed roots growing into intact sediments hosting a well-established microbial community.

**Planar optodes**—The setup for planar  $O_2$  measurements has previously been described in detail (Glud et al. 1996; Holst et al. 1998) and is only presented briefly below. The planar optode consisted of an  $O_2$  quenchable ruthenium luminophore embedded in plasticized vinyl that was immobilized on a  $175\text{-}\mu\text{m}$ -thick transparent support foil (Glud et al. 1996). Excitation light was supplied by blue-light-emitting diodes  $\lambda = 470 \text{ nm}$  (Nichia), equipped with an emission

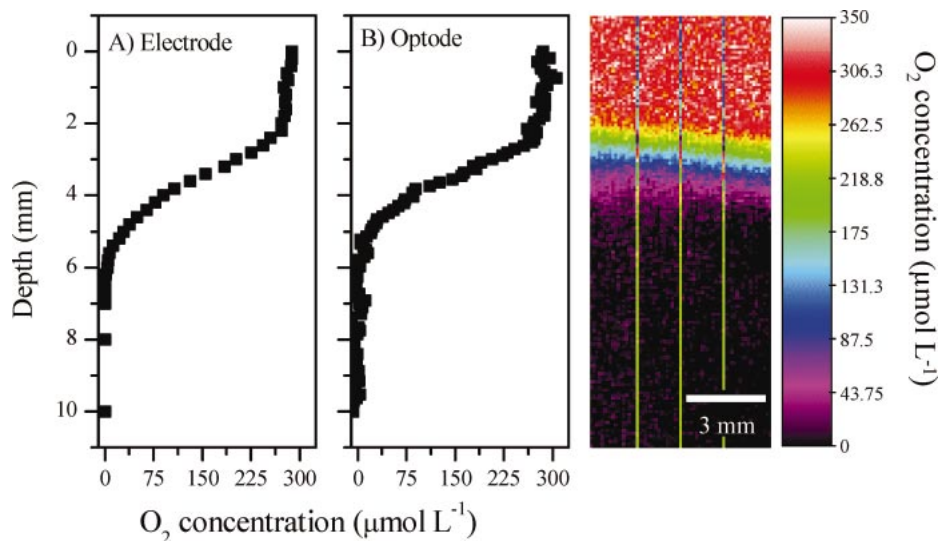


Fig. 2. Comparison of oxygen profiles made by microelectrode and extracted from the planar optode image to the right. Both profiles are an average of three profiles. The optode O<sub>2</sub> profiles are indicated by yellow lines in the oxygen image and the electrode profiles were measured about 1 cm behind these lines.

filter (Unaxis C-54, Linos). Images of the O<sub>2</sub> quenchable excitation light were obtained by a digital charge coupled device camera (SensiCam, PCO Computer Optics) equipped with a 25 mm/1.4 Nikon wide-angle lens (Fig. 1). The peltier cooled camera chip consisted of 640 × 480 pixels and, at the given optical configuration, the obtained images covered an area of 6.0 × 4.5 cm at a spatial resolution of 93 × 93 μm. In the present study, we used lifetime-based imaging to quantify the O<sub>2</sub> distribution in front of the planar optode. The sensors were calibrated using a modified Stern–Volmer equation accounting for the presence of a nonquenchable fraction of luminescence light ( $\alpha$ ) (Holst et al. 1998):

$$\frac{\tau}{\tau_0} = \alpha + \frac{1}{1 + K_{SV}C}(1 - \alpha) \quad (1)$$

where  $\tau$  and  $\tau_0$  represent the luminescent lifetime at an O<sub>2</sub> concentration of  $C$  and at anoxia, respectively.  $K_{SV}$  is the quenching coefficient of the luminophore and, for  $\alpha$ , we applied an image constant of 0.2. Thus a two-point calibration of the images using signals obtained at 100% and 0% air saturation was sufficient for later image calibration using Eq. 2:

$$C = \frac{\tau_0 - \tau}{K_{SV}(\tau - 0.2\tau_0)} \quad (2)$$

Images of the luminescent lifetime ( $\tau$ ) were calculated by rationing images of luminescent signals obtained in two well-defined time frames on the luminescent decay curve. For further details on the measuring scheme, we refer to Holst et al. (1998). The lifetime-based measuring scheme made it possible to apply transparent optodes without any optical insulation (Holst and Grünwald 2001). Thereby, the sediment structure and root position could be followed directly through the planar optode in parallel to the O<sub>2</sub> measurements. The entire planar optode setup was covered by

black cloth and O<sub>2</sub> images were only obtained after switching off the ambient light to avoid any potential impact on the luminescent signals (so-called light measurements, e.g., Figs. 3 and 4 were obtained immediately after eclipse of the ambient light).

*Measuring setup*—The oxygen leakage of the plant roots was investigated as a function of the imposed irradiance and the O<sub>2</sub> concentration of the overlying water (Fig. 1). The ambient light source was a fiber-optic tungsten/halogen lamp (KL 2500 Schott) equipped with a diffuser head to obtain a homogenous light field around the plants. The absolute irradiance level was determined by a Licor LI-1000 light meter. The O<sub>2</sub> of the overlying water phase was either maintained at air saturation by flushing with an air pump or during experiments with variable O<sub>2</sub> concentration regulated by flushing with an O<sub>2</sub>/N<sub>2</sub> or air/N<sub>2</sub> gas mixture controlled from a 2-channel digital gas mixer (Brooks 0154). During experiments, the oxygen concentration of the overlying water was followed continuously by a calibrated Clark-type O<sub>2</sub> microelectrode (Revsbech 1989).

Complementary O<sub>2</sub> microprofiles at the sediment–water interface (SWI) were measured by microelectrodes having an outer diameter <5 μm, a stirring sensitivity <2%, and response time of <2 s (Revsbech 1989). The sensors were positioned by a micromanipulator and the sensor current was measured by a picoammeter (Unisense 2000) connected to a strip-chart recorder. The profiles had two inherent calibration points, measured in the overlying water and the anoxic sediment layers.

The O<sub>2</sub> penetration depth at the primary SWI was determined directly from the microprofiles accounting for the diffusive boundary layer (DBL) thickness (Jørgensen and Revsbech 1985). The diffusive O<sub>2</sub> uptake (DOU) was calculated from Fick's first law of diffusion;  $DOU = D_0 dC/dz$ , where

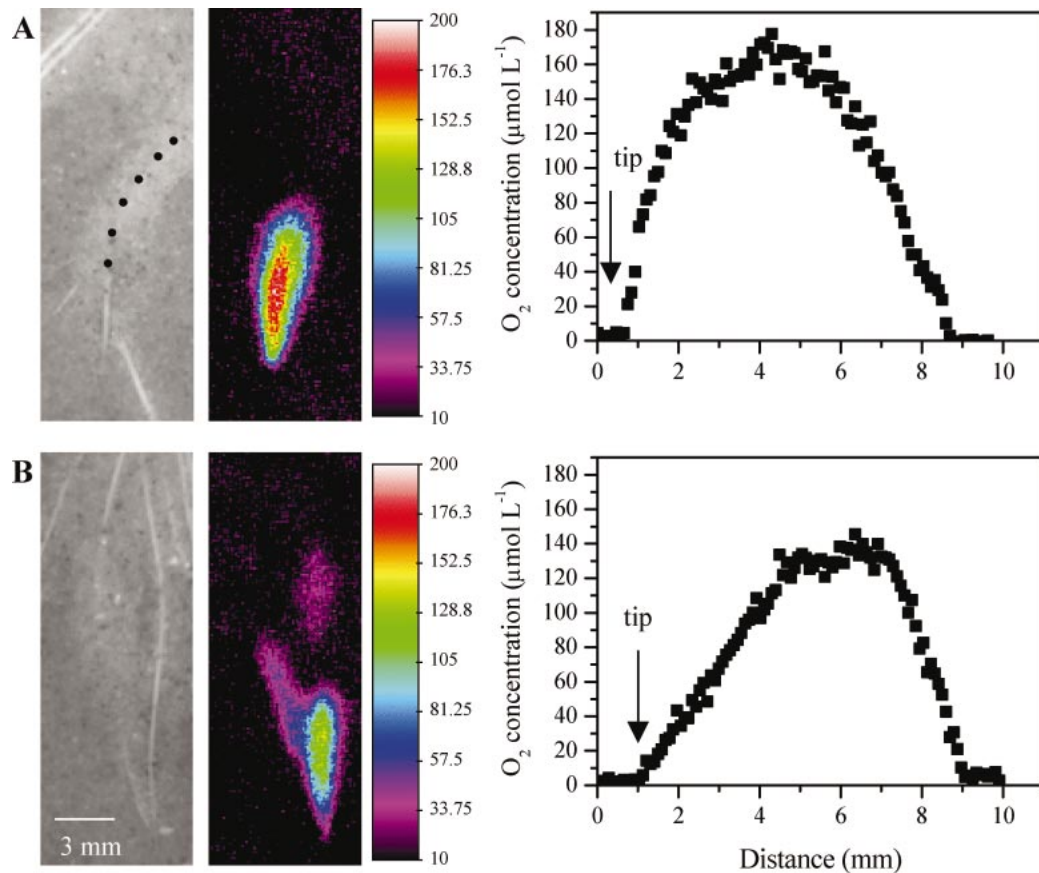


Fig. 3. Oxygen distribution around roots from two *Z. marina* plants (A and B) at light intensity above photosynthetic saturation ( $500 \mu\text{mol photons m}^{-2} \text{s}^{-1}$ ). For each plant, the root distribution is shown in the black-and-white image (left), where roots appear as white lines (marked by black dots). Planar optode images of oxygen distribution are shown in the middle and peak oxygen concentrations along the root length axis starting from the root tip are shown to the right. The optode image in B also shows the interference of oxygenated zones from two other, deeper lying roots not visible in the black-and-white photo.

$D_0$  is the molecular diffusion coefficient for  $\text{O}_2$  at the given temperature and salinity, and  $C$  is the oxygen concentration at depth  $z$  within the DBL (Jørgensen and Revsbech 1985). The average volume-specific  $\text{O}_2$  consumption,  $R_{\text{SWI}}$ , was calculated as  $R_{\text{SWI}} = \text{DOU}/\text{O}_2$  penetration depth.

As  $\text{O}_2$ -leaking roots of the plants continuously grew into otherwise anoxic sediment, the potential volume-specific  $\text{O}_2$  consumption,  $R_{\text{sed}}$  for these layers was determined in a similar fashion. After gentle removal of the upper sediment layers, allowing air-saturated water to get in contact with the newly exposed sediment,  $\text{O}_2$  microprofiles were measured at a regular interval for 11 h. The potential  $R_{\text{sed}}$  of the deeper sediment layers was then calculated as described above.  $R_{\text{sed}}$  for these sediments was also estimated by slurry incubations. Here, 10 g of sediment from 4 cm depth was added to a Winkler bottle containing air-saturated water. The bottle was sealed with a microelectrode tip penetrating the lid to follow the  $\text{O}_2$  concentration decrease while the sediment was kept in suspension by a rotating magnet bar. Sediment porosity ( $\phi$ ) was determined by drying sediment to constant weight at  $110^\circ\text{C}$  and the organic matter content was expressed by loss of ignition after 5 h at  $520^\circ\text{C}$ .

## Results

**Sediment and plant characteristics**—The sediment hosting the investigated plants was characterized as sandy silt with a low porosity and low organic carbon content (Table 1). The  $\text{O}_2$  penetration depth at the SWI, the DOU, and the volume-specific respiration were in the range of typical coastal sediments (e.g., Glud et al. 2003), and the  $\text{O}_2$  penetration depth obtained by the two techniques aligned very well (Table 1 and Fig. 2). This indicates that any potential smearing of the  $\text{O}_2$  distribution caused by lateral diffusion of  $\text{O}_2$  within the optical sensor was negligible.

In order to estimate the potential volume-specific aerobic respiration rate,  $R_{\text{sed}}$ , in the deeper sediment layers experiencing transient  $\text{O}_2$  leakage from the plant roots  $\text{O}_2$  microprofiles were measured after removing the upper 1–3 cm of sediment and exposing the new SWI to air saturated overlying water. The average volume-specific  $\text{O}_2$  consumption ( $R_{\text{sed}}$ ) in the gradually expanding oxic zone remained constant for 11 h and was similar to the equivalent value derived from the primary interface (Table 1). The potential  $R_{\text{sed}}$  value quantified from slurry incubations was 1.4 times larger than

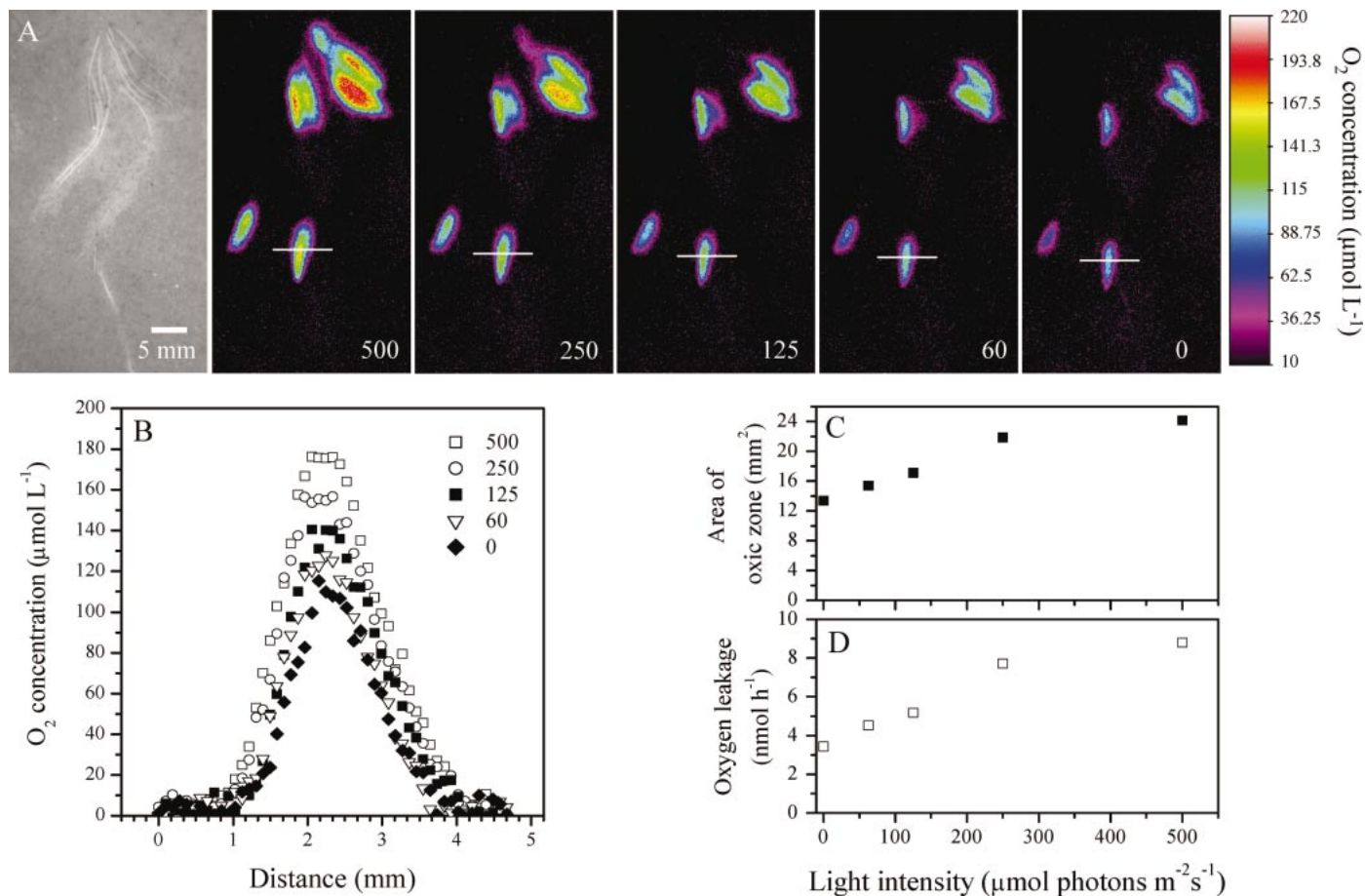


Fig. 4. Oxygen distribution around roots at different light intensities. (A) Planar optode images of O<sub>2</sub> concentrations around the roots at light intensities ranging from 0 to 500  $\mu\text{mol photons m}^{-2} \text{s}^{-1}$ . (B) Horizontal profiles of O<sub>2</sub> concentration extracted from the O<sub>2</sub> images at the different light intensities. Each profile represents an average of 10 profiles extracted at the center of the oxygen-excreting part of the root (indicated by white lines in A). (C) Area of oxygenated sediment around the root as a function of light intensity. (D) Oxygen leakage from the root as a function of light intensity estimated by combining the volume of oxygenated sediment by the root with sediment oxygen-consumption rate.

the average value calculated from the intact sediment with diffusive mediated O<sub>2</sub> transport. The investigated plants were relatively small but typical for Danish waters, and their basic characteristics measured after the experiments were very similar (Table 2).

*Oxygen dynamics as a function of irradiance*—Oxygen release from actively growing roots was confined to a small

region extending from the root tip to ~6–8 mm up the root (Fig. 3). The oxygen concentration up along the root increased to a maximum value at ~2–4 mm behind the root tip, and this region was also characterized by the maximum width of the oxic area, indicating that this zone represented the root section with maximum oxygen leakage (Fig. 3). This overall pattern was apparent for all investigated plants and at all the applied irradiance levels.

Table 1. Basic characteristics of the sediment  $\pm$  SD.

Porosity (vol vol <sup>-1</sup> )	0.36 $\pm$ 0.01	<i>n</i> =3
LOI (%)	0.25 $\pm$ 0.02	<i>n</i> =3
O <sub>2</sub> penetration depth (mm) ME*	2.9 $\pm$ 0.04	<i>n</i> =3
O <sub>2</sub> penetration depth (mm) PO†	3.0 $\pm$ 0.12	<i>n</i> =3
DOU (mmol m <sup>-2</sup> h <sup>-1</sup> ) ME	18.8 $\pm$ 2.6	<i>n</i> =3
<i>R</i> <sub>swi</sub> (nmol cm <sup>-3</sup> s <sup>-1</sup> ) ME	0.072 $\pm$ 0.015	<i>n</i> =3
<i>R</i> <sub>sed</sub> (nmol cm <sup>-3</sup> s <sup>-1</sup> ) ME	0.082 $\pm$ 0.032	<i>n</i> =7
<i>R</i> <sub>sed</sub> (nmol cm <sup>-3</sup> s <sup>-1</sup> ) slurry incubation	0.118 $\pm$ 0.004	<i>n</i> =2

\* ME, microelectrode derived.

† PO, planar optode derived.

Table 2. Basic plant characteristics  $\pm$  SD.

Root length (cm)	6.3 $\pm$ 0.8	<i>n</i> =5
Root diameter (mm)	0.39 $\pm$ 0.02	<i>n</i> =5
Root growth rate (mm d <sup>-1</sup> )	8.7 $\pm$ 1.7	<i>n</i> =2*
Roots internode <sup>-1</sup>	11 $\pm$ 1	<i>n</i> =5
Rhizome internode length (cm)	0.9 $\pm$ 0.2	<i>n</i> =5
Rhizome diameter (mm)	2.5 $\pm$ 0.2	<i>n</i> =5
No. of leaves	5	<i>n</i> =5
Leaf length (cm)	26.6 $\pm$ 5.2	<i>n</i> =5
Leaf width (mm)	2.6 $\pm$ 0.3	<i>n</i> =5

\* Based on three replicates from each of two plants.

Plants were exposed to gradually decreasing irradiance to evaluate the impact of light on the oxygen leakage from the roots. Measurements were initiated at  $500 \mu\text{mol photons m}^{-2} \text{ s}^{-1}$  (maximum irradiance) and continuous imaging documented that quasi-steady state in  $\text{O}_2$  distribution was reached  $\sim 1$  h after change of the irradiance. For practical reasons, a time interval of 2 h at each irradiance level was chosen. As the plants were exposed to decreasing irradiance, the size of the oxic area and the  $\text{O}_2$  concentrations of the oxic zone decreased (Fig. 4). The maximum oxygen concentration at the root surface dropped from  $175 \mu\text{mol L}^{-1}$  to  $115 \mu\text{mol L}^{-1}$ , when the irradiance changed from  $500 \mu\text{mol photons m}^{-2} \text{ s}^{-1}$  to darkness (Fig. 4A,B). Hence, the investigated plants were able to maintain oxic conditions around their root tip even without active photosynthesis.

The maximum width of the oxic area, as resolved by the  $\text{O}_2$  images, ranged from 2.5 mm in darkness to 3.7 mm at maximum irradiance. In areas where roots were closely packed, the oxic zones fused into larger oxic areas of 10–20  $\text{mm}^2$  (e.g., Fig. 4). The total oxygenated area in the optode images increased linearly with irradiance in the interval of 0–250  $\mu\text{mol photons m}^{-2} \text{ s}^{-1}$ , but the leakage rate tended to saturate at maximum irradiance (Fig. 4C). The  $\text{O}_2$  consumption rate of sediment around the investigated roots was calculated from the microelectrode-derived volume-specific respiration ( $R_{\text{sed}}$ ) and the oxic volume around each root; the latter was estimated by assuming a hemispheric  $\text{O}_2$  distribution around the roots growing along the planar optode. The calculations showed that total oxygen release from the root tip selected in Fig. 4A ranged from  $8.81 \text{ nmol h}^{-1}$  at light-saturated photosynthesis to  $3.44 \text{ nmol h}^{-1}$  in darkness (Fig. 4D). The values varied among the individual root tips, but accounting for the six root tips visible in Fig. 4, the average oxygen release per root amounted to  $3.10 \pm 1.70 \text{ nmol h}^{-1}$  and  $7.09 \pm 0.89 \text{ nmol h}^{-1}$  in darkness and at saturating light conditions, respectively. Other investigated plants incubated at slightly variable light conditions gave very similar results (data not shown). During all of these measurements, continuous air flushing kept the  $\text{O}_2$  concentration of the overlying water at 100% air saturation ( $280 \mu\text{mol L}^{-1}$ ).

*Oxygen dynamics as a function of  $\text{O}_2$  concentration in the overlying water phase*—The oxygen leakage from the roots of plants that were kept in darkness was closely related to the oxygen concentration of the overlying water column. Lowering the  $\text{O}_2$  concentration in the water column from  $280 \mu\text{mol L}^{-1}$  (air saturation level) to  $155 \mu\text{mol L}^{-1}$  in darkness caused an 86% decrease in the area of the oxygenated zone and a 94% decrease in the calculated  $\text{O}_2$  leakage (Fig. 5A,C,D). As the  $\text{O}_2$  concentration was lowered to  $70 \mu\text{mol L}^{-1}$ , the oxygenated area completely vanished. Oxygen concentrations at the root surface in darkness derived from horizontal  $\text{O}_2$  profiles ranged from  $102 \mu\text{mol L}^{-1}$  to  $20 \mu\text{mol L}^{-1}$  to below detection limit at water column  $\text{O}_2$  concentrations of  $280 \mu\text{mol L}^{-1}$ ,  $155 \mu\text{mol L}^{-1}$ , and  $70 \mu\text{mol L}^{-1}$ , respectively (Fig. 5B). This strongly indicated that  $\text{O}_2$  leakage completely ceased at  $\text{O}_2$  concentrations  $< 70 \mu\text{mol L}^{-1}$ . When the  $\text{O}_2$  concentration in the water column returned to  $280 \mu\text{mol L}^{-1}$ , the oxygenated areas restored and the area

only expanded slightly by additional light exposure ( $250 \mu\text{mol photons m}^{-2} \text{ s}^{-1}$ ), when the overlying water was continuously air flushed.

A similar experiment was performed on a younger root set, but here the  $\text{O}_2$  concentration of the overlying water was raised to  $450 \mu\text{mol L}^{-1}$  in darkness. Under these extreme conditions, small amounts of oxygen leaked out from regions of a root that previously appeared impermeable to  $\text{O}_2$ , indicating that the barrier to ROL in some sections was imperfect at extreme internal  $\text{O}_2$  tensions (Fig. 6).

*Oxygen release as a function of root growth and rhizosphere development*—The rhizosphere structure was very dynamic and substantial root development occurred on short time scales (Fig. 7). The growth rate of roots calculated from times series of black-and-white images obtained in parallel to the  $\text{O}_2$  images ranged from  $6.9 \text{ mm d}^{-1}$  to  $11.5 \text{ mm d}^{-1}$ . There was no significant difference in root growth during light or dark, and average diel growth rates amounted to  $8.7 \text{ mm d}^{-1}$  (Table 1). Interestingly, the oxygenated zones clearly changed with the root age (Fig. 7). As the roots progressively aged, the width, the length, and the maximum  $\text{O}_2$  concentration of the oxic area decreased. An example is shown in Fig. 8, where changes in the oxygen release from two roots moving in parallel through the sediment (see Fig. 7) were followed for 41 h. Considerable variation occurred over the time sequence, with significant differences between light and dark periods and a general trend of decreasing oxygen release as the roots aged and moved deeper into the sediment. During day time, the rate of  $\text{O}_2$  leakage varied, probably reflecting variation in internal  $\text{O}_2$  concentrations.

Combining information on root growth rates with root lengths suggests that roots stopped growing after 7.3 d ( $\text{SD} \pm 0.9 \text{ d}$  at  $250 \mu\text{mol photons m}^{-2} \text{ s}^{-1}$  and 100% air saturation of overlying water) and the  $\text{O}_2$  leakage eventually ceased. The growing roots left light-colored oxidized tracks in the otherwise reduced sediment, which appeared stable for several days to weeks (data not shown).

## Discussion

*$\text{O}_2$  leakage from plant roots as studied by planar optodes*—The present investigation represents a detailed two-dimensional study on  $\text{O}_2$  leakage from plant roots. The oxic environment around root tips of *Z. marina* proved to be extremely dynamic both spatially and temporally. The rate of  $\text{O}_2$  leakage in a given sediment depended on the irradiance, the  $\text{O}_2$  concentration of the overlying water phase, and the root age. Further, the oxic microniches continuously moved along with the actively growing roots. To map this extensive dynamic would be extremely difficult with any other technique, and planar optodes thereby complement and overcome some of the problems of previously applied techniques. However, the technique has the inherent problem that measurements are performed along a glass plate.

Jensen et al. (2005) tested the potential of planar optodes for rhizosphere studies and measured the extent of the oxygenated zone of *Z. marina* roots both with microelectrodes and planar optodes. They found that the width of the oxic area displayed by the  $\text{O}_2$  images was up to approximately

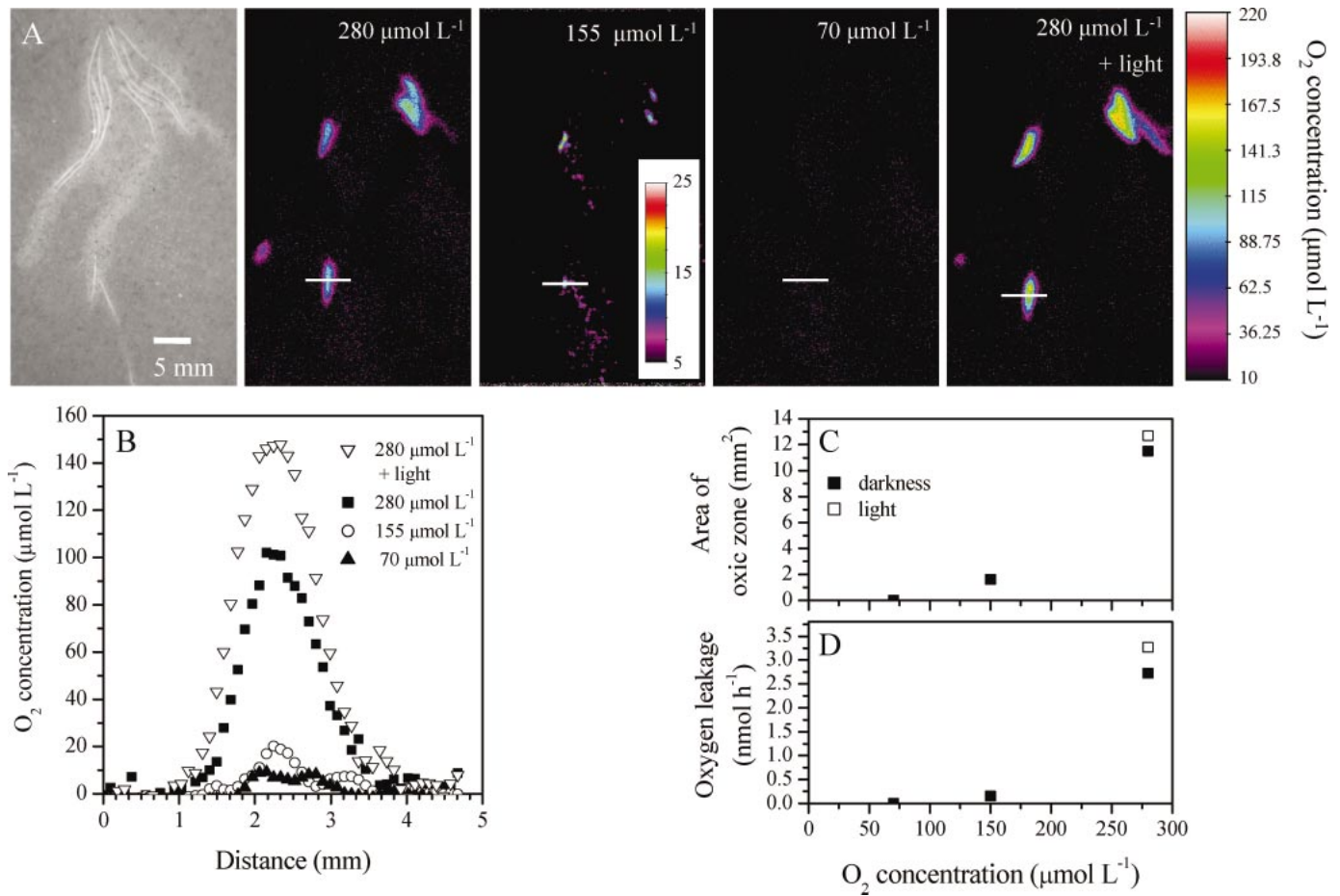


Fig. 5. Changes in oxygen distribution around roots at different  $O_2$  concentrations in the water column starting at 280  $\mu\text{mol L}^{-1}$ , decreasing to 155 and 70  $\mu\text{mol L}^{-1}$ , and ending again at 280  $\mu\text{mol L}^{-1}$  but with the plant illuminated (250  $\mu\text{mol photons m}^{-2} \text{ s}^{-1}$ ). (A) Planar optode image of root zone  $O_2$  concentrations. Note the change of scale at 155  $\mu\text{mol L}^{-1}$ . (B) Horizontal profiles of  $O_2$  concentration extracted from the  $O_2$  images at different  $O_2$  concentrations in the water column. Each profile represents an average of 10 profiles extracted at the center of the oxygen-excreting part of the root (indicated by white lines in A), except at 155  $\mu\text{mol L}^{-1}$ , where only three profiles were extracted due to the limited extension of the oxygen excretion zone. (C) Area of oxygenated sediment around the root as a function of  $O_2$  concentration in the water column. (D) Oxygen leakage from the root as a function of  $O_2$  concentration in the water column, estimated by combining the volume of oxygenated sediment by the root with sediment oxygen-consumption rate.

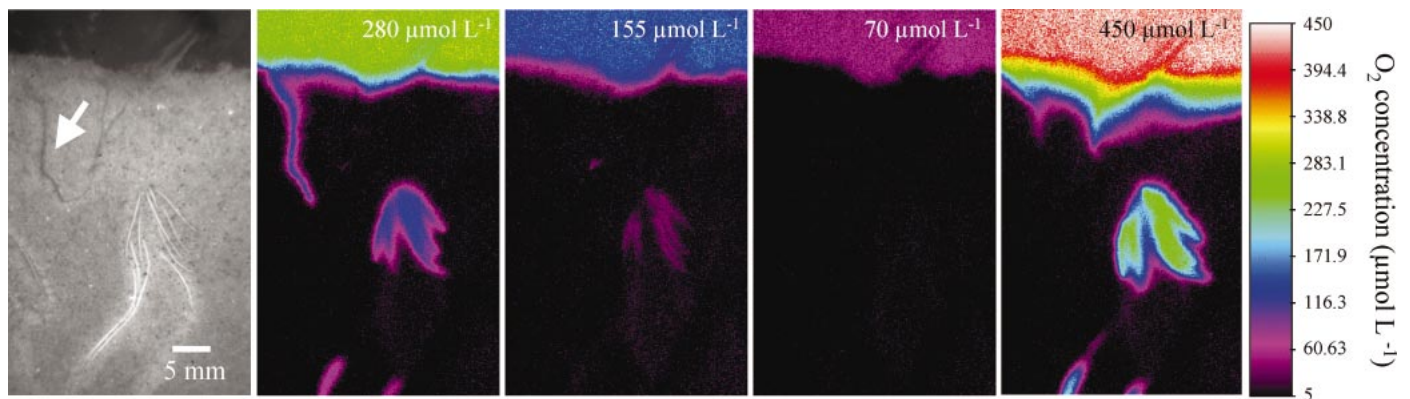


Fig. 6. Planar optode images illustrating changes in oxygen distribution around roots when  $O_2$  concentrations in the water column decrease from 280  $\mu\text{mol L}^{-1}$  to 155  $\mu\text{mol L}^{-1}$  and 70  $\mu\text{mol L}^{-1}$ , and finally increase to 450  $\mu\text{mol L}^{-1}$ . The black part of the black-and-white photograph is the water column and the grey part is sediment. A worm burrow is indicated by an arrow in the upper left part of the images.

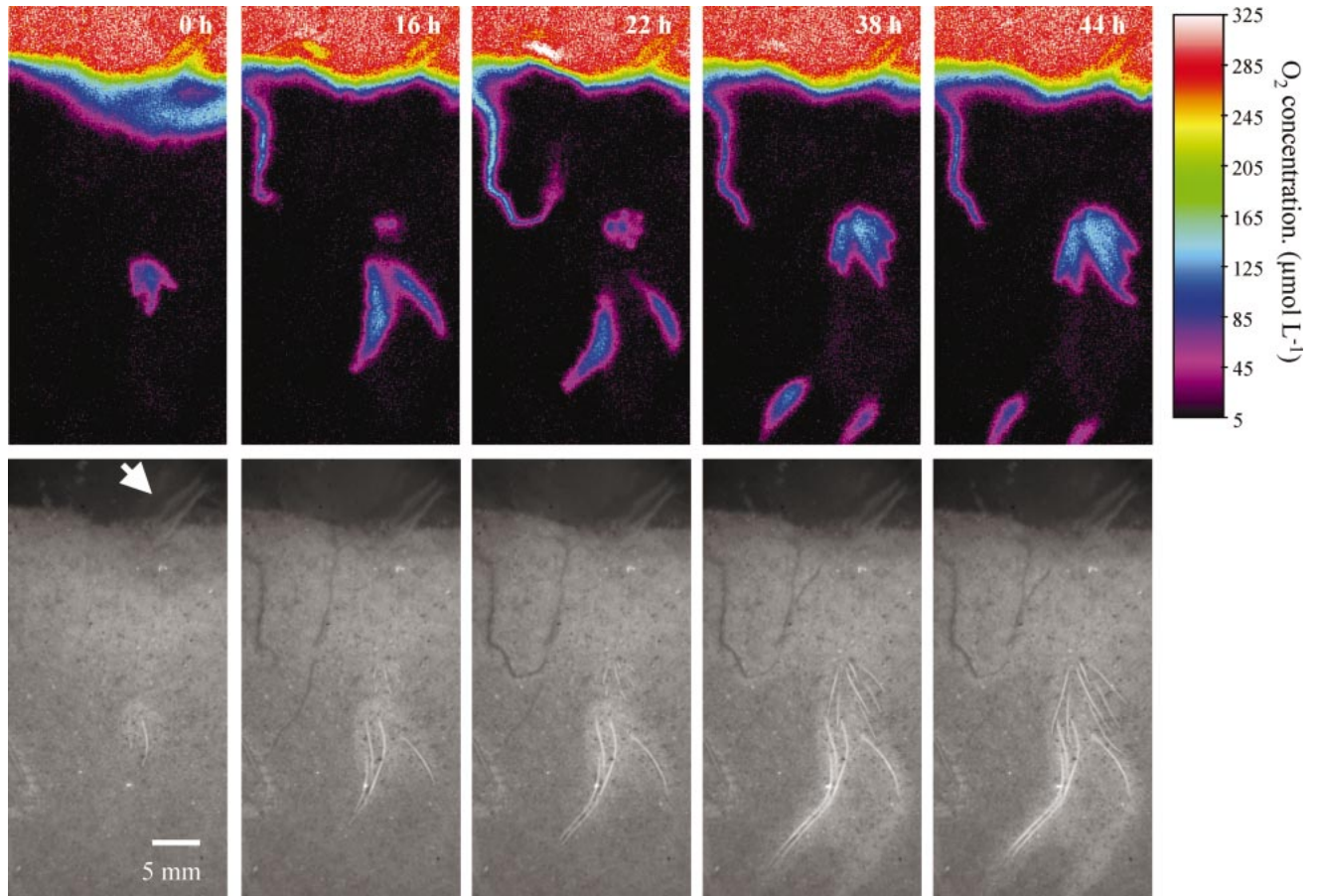


Fig. 7. Changes in rhizosphere oxygenation (upper panel) and root development (lower panel) of *Z. marina* over 44 h. Images were taken during darkness. A worm burrow developed after 16 h (upper left part of the images). Remains of an old leaf still attached to the rhizome is indicated by an arrow in the first black-and-white photograph in the series.

two times larger than the diameter of the oxic zone as quantified by microelectrodes. This suggested that placing an  $O_2$  impermeable barrier along the root enlarges the  $O_2$  area compared with a situation without the presence of a wall. However, the pioneering study of Jensen et al. (2005) is not directly comparable with the present study. The measurements that compared the two techniques were not performed in the

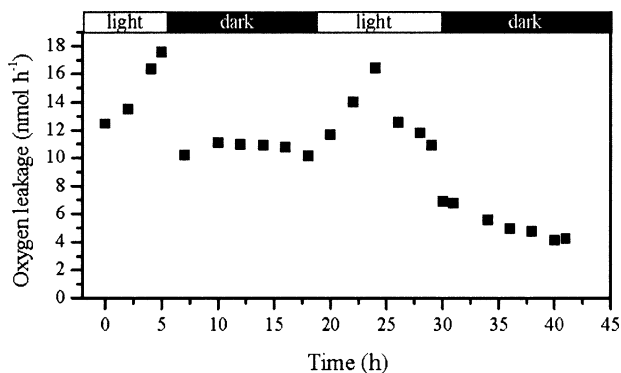


Fig. 8. Temporal changes in total oxygen leakage from two developing roots of *Z. marina*. Periods of light and darkness are indicated above the figure.

same sediment (or on the same root), roots were placed and fixed by strings along the planar sensors before they were covered by sediment and subsequently  $O_2$  measurements were performed. However, more importantly, they applied intensity-based imaging and, thus, it was necessary to optically insulate the sensing chemistry with a layer of 40- $\mu\text{m}$  black silicone (Glud et al 1996). Silicone is highly permeable to  $O_2$  (Gundersen et al. 1998) and the silicone layer could have caused lateral diffusion inside the sensor and enlargement of the original  $O_2$  area of the plane in front of the sensor. This potential problem was avoided in the present study using lifetime-based imaging and, hence, the optical insulation could be avoided (Holst and Grünwald 2001). In addition to minimizing any potential smearing problem (Fig. 2), it also allowed us to use transparent optodes, facilitating the alignment between roots and the imaged  $O_2$  distribution.

We assumed that the  $O_2$  was hemispherically distributed around roots growing along a wall. This was a reasonable assumption and parallel to the general assumption of radial outward  $O_2$  diffusion from roots fully surrounded by sediment (e.g., Armstrong 1971). The maximum radius of the oxygenated zone of the present study ranged between 1.4 mm in darkness and 2.1 mm at maximum irradiance. As outlined above, these values overestimated the radius of the

oxic zone around root tips not growing along the planar optode (Jensen et al. 2005). The radius of the oxic zone around root tips in the interior of the aquarium can be approximated by assuming that the total oxic volume around the roots (or the O<sub>2</sub> leakage) is unaffected by the vicinity of a wall at quasi-steady state. Thereby, the oxic volumes around the root tips in the two situations are identical and simple geometric calculations then show that the width of the oxic area overestimates the radius of the oxic zone surrounding plant roots in the interior of the aquaria by a factor 2<sup>0.5</sup> (=1.4). Thus, it follows that the estimated oxic radius around plant roots not affected by the planar geometry ranged between 1.0 and 1.5 mm. This aligns with microsensor measurements on *Z. marina* roots, where the radius was estimated to be ~1 mm at saturating light conditions (Jensen et al. 2005), which is considerably larger than the 80 μm found for the seagrass *Cymodocea rotundata* (Pedersen et al. 1998). However, the oxygen demand of the sediments applied in the different studies has large implications for the size of the resolved oxic zones and compromises any direct comparison. The validity of the assumption that O<sub>2</sub> leakage from root tips was only marginally affected by the vicinity of a wall is presently being investigated by modeling approaches and various experimental setups. The task is not trivial but, a priori, it seems like a reasonable approximation given the efficient internal O<sub>2</sub> transport rates of *Z. marina* (Greve et al. 2003; Pedersen et al. 2004). The  $R_{\text{sed}}$  used to estimate oxygen release from the roots do not account for any stimulated activity following potential leakage of labile organic material from the root tips (e.g., Moriarty et al. 1986). Further, we cannot exclude any potential physiological change of roots growing along a wall as compared with being fully surrounded by sediment.

*Influence of irradiance and water-column oxygen concentrations for rhizosphere oxygen dynamics*—Oxygen release from *Z. marina* roots was restricted to a small fraction of the total root length. The presence of a barrier to ROL is well known for wetland plants, such as *Phragmites australis* (Armstrong et al. 2000), *Oryza sativa* (Armstrong 1971; Colmer 2003), *Hordeum marinum* (McDonald et al. 2001), but has only recently been demonstrated for *Z. marina* (Jensen et al. 2005), and the findings are confirmed by the present study. Apart from restricting oxygen loss, the barrier may also act as a barrier to invasion of phytotoxins and may also have negative effects by reducing the permeability toward nutrient uptake (Barnabas 1996). So far, the barrier to ROL has only been documented for two seagrass species, *Z. marina* and *Halophila ovalis* (Connell et al. 1999; Jensen et al. 2005), but the structures suggested to be responsible for the barrier to ROL (Casparian bands, suberin lamellae) have been observed in several seagrass species, such as *Zostera* sp. (several species), *Ruppia maritima* (Barnabas 1996), *Halodule uninervis* (Barnabas 1994a), and *Phyllospadix scouleri* Hook (Barnabas 1994b). Even though our conclusions only can be extended to *Z. marina*, a barrier to ROL seems to be a general phenomenon in seagrasses. Current work is presently investigating rhizosphere O<sub>2</sub> dynamics on a range of seagrasses using the planar optode approach.

The oxygen release from root tips of *Z. marina* increased

linearly with the irradiance until saturation was reached at the maximum light intensity. This aligns well with previous studies suggesting that the photosynthetic activity of the leaves regulates the ROL of seagrasses via the internal O<sub>2</sub> concentration (Sand-Jensen et al. 1982; Pedersen et al. 1998; Connell et al. 1999). The estimated amount of oxygen released per root decreased 61.1% from light to darkness, which was similar to results obtained with microelectrodes for *Z. marina* and *C. rotundata*, where the ROL decreased 55.0% and 56.6%, respectively (Pedersen et al. 1998; Jensen et al. 2005). All of these studies thus indicate that 100% air saturation in darkness enable seagrasses to maintain an oxic sphere around their root tips in relatively active sediments (Table 1; Pedersen et al. 1998; Jensen et al. 2005).

The meristem and rhizome O<sub>2</sub> concentration is closely coupled to O<sub>2</sub> concentration of the overlying water column (Greve et al. 2003; Pedersen et al. 2004; Borum et al. 2005). In the present study, the oxygenated sphere around the root disappeared at water column O<sub>2</sub> concentrations between 70 and 150 μmol L<sup>-1</sup> and left no protection against invasion of phytotoxic compounds such as sulfide, which have been shown to seriously affect seagrass survival (Holmer and Bondgaard 2001). Sulfide invasion has been demonstrated to occur in *Z. marina* and *Thalassia testudinum* in darkness at low oxygen concentrations in the water column (Pedersen et al. 2004; Borum et al. 2005). Situations of low oxygen concentrations in the water column are not unusual in natural seagrass beds and are often accompanied by severe seagrass mortality. The presence of a well-functioning oxic microshield around the roots is therefore of vital importance for seagrasses.

Increasing the O<sub>2</sub> concentrations in the water column to 450 μmol L<sup>-1</sup> (160% air saturation) increased both the extent and the peak O<sub>2</sub> concentrations of the oxygenated zones around the root tips. The sections of the roots affected by ROL also increased, showing that even the relatively impermeable sections of the roots may leak O<sub>2</sub> during extreme internal O<sub>2</sub> tensions. This situation may arise under natural conditions in areas with high pelagic or benthic primary production. In one of our initial experiments, the dark cover of the aquaria wall was removed and benthic diatoms developed at the sediment surface, forming a surface layer of elevated O<sub>2</sub> concentrations (~600 μmol L<sup>-1</sup> at 300 μmol photons m<sup>-2</sup> s<sup>-1</sup>). During such situations, the peak oxygen concentrations at the root surface increased to 260 μmol L<sup>-1</sup>, even though the water column was kept at 100% air saturation (280 μmol L<sup>-1</sup>) (data not shown). This indicates that the basal part of the shoot is permeable to O<sub>2</sub> and that microphytobenthos photosynthesis around the plant base can induce enhanced O<sub>2</sub> leakage from the rhizosphere.

The rhizosphere of *Z. marina* was highly dynamic, with extensive root development occurring on short time scales. The oxygen excretion from roots decreased with root age, as demonstrated in the planar optode images in Fig. 7, where the O<sub>2</sub> distribution around both young and old roots is shown, and in Fig. 8, showing the temporal changes in O<sub>2</sub> excretion from two developing roots. This could partly be a consequence of increased transport distance from the leaves to the root tips as roots grew older but could also be related to increasing impermeability toward ROL in older, less ac-

tive roots. Hence, the  $O_2$  dynamic in a seagrass rhizosphere is highly variable and depends both on light availability, root age, oxygen concentration in the water column (and thus ventilation of the bed), and potential benthic diatom covers.

*Seagrass influence on benthic  $O_2$  exchange sediment biogeochemistry*—In order to quantify the importance of ROL to the total benthic  $O_2$  consumption in the sediment, we extrapolated the findings from root tips growing along the wall (see previous) to all plant roots of the aquaria. Assuming a 12:12 LD cycle and that oxygen was leaking from roots on the first two internodes (each containing 11 roots) resulted in a total oxygen loss of  $2.69 \mu\text{mol } O_2 \text{ plant}^{-1} \text{ d}^{-1}$ . These results were extrapolated to the scale of seagrass beds by using a shoot density of  $905 \text{ shoots m}^{-2}$ , representing the average shoot density at 29 locations in temperate regions of the northern hemisphere (Olesen and Sand-Jensen 1994). The oxygen release from the rhizosphere of a typical *Z. marina* bed in the investigated sediment thus amounted to  $2.28 \text{ mmol m}^{-2} \text{ d}^{-1}$ . This corresponded to  $\sim 12\%$  of the diffusive oxygen uptake over the sediment–water interface, which is in the same range as extrapolated from the microsensor study of Jensen et al. (2005), where the ROL ranged from 2% to 14% of DOU. In contrast, Pedersen et al. (1998, 1999) found the oxygen loss from *Cymodocea rotundata* to be of the same magnitude as the DOU. Their estimate was, however, based only on a few point measurements along the roots and on the assumption that ROL occurred along the entire root length of *C. rotundata*. The present study documents the extreme temporal dynamics of oxygen leakage from *Z. marina* roots (e.g., Fig. 8), and extrapolation from simple photosynthesis-irradiance (PE) relations (Fig. 4C) could represent an oversimplification. A more correct estimate was made by integrating and extrapolating the temporal dynamics presented in Fig. 8 to average beds as outlined above. This resulted in a total rhizospheric oxygen loss of  $2.48 \text{ mmol m}^{-2} \text{ d}^{-1}$ , which is very close to the estimate based on the PE relation. For comparison with other interfaces, the average ROL can also be expressed per area of the permeable root tip. The value can be roughly estimated by dividing the total  $O_2$  release rate with the area of root tip surface or, more correctly, by using a simple equation for radial diffusion:  $J = \phi R_{\text{sed}} L / (L/2A + 1)$  (Fenchel 1996), where  $L$  equals the  $O_2$  penetration depth from the root (i.e., 1–1.5 mm) and  $A$  the average root diameter. The latter approach gave slightly lower results, being very dependent upon the absolute value of the porosity; however, the results ranged between  $\sim 7$  and  $11 \text{ mmol m}^{-2} \text{ d}^{-1}$  in darkness and  $\sim 12$  and  $22 \text{ mmol m}^{-2} \text{ d}^{-1}$  at saturating light conditions. These values are in the lower end of radial  $O_2$  release from burrows of, e.g., small polychaetes (e.g., Fenchel 1996; Wenzhöfer and Glud 2004).

Nevertheless, the overall ROL of seagrasses seems to be of minor importance for total benthic  $O_2$  uptake (TOU) of coastal sediments as compared with, for instance, fauna-mediated  $O_2$  uptake, which typically range between 25% and 50% of the TOU (Glud et al. 2003; Meile and van Cappellen 2003) or pressure-induced percolation of the interstice of sandy environments (Precht et al. 2004; de Beer et al. 2005). However, the transient ROL of seagrasses induce a local

small-scale biogeochemical heterogeneity that could have importance for the sulfide buffer capacity and the coupled nitrification–denitrification activity of marine sediments. But so far, it has not been possible to document any significant effect of rhizosphere dynamics on coupled denitrification (Risgaard-Petersen et al. 1998). The reason might be that plants compete efficiently with nitrifying bacteria for ammonium (Verhagen et al. 1994). But more likely, the extreme dynamics of the ROL documented in the present study may prevent the slow-growing nitrifying bacteria from reaching quantitatively important population densities in the short-lived transient oxic microniches.

Sulfate reduction rates are stimulated in seagrass-inhabited sediments presumably due to the excretion of organic compounds from the roots and due to the general accumulation of organic material in seagrass beds (e.g., Isaksen and Finster 1996; Holmer and Nielsen 1997; Pollard and Moriarty 1991). As sulfate reduction occurs under anaerobic conditions, the oxygen leakage from the roots should inhibit this process, but the sulfate-reducing bacteria have been found living directly on the root surface (Blaabjerg et al. 1998). The explanation for this apparent discrepancy is probably that sulfate-reducing bacteria colonize the regions of the root where the barrier to ROL has been established and thereby avoid being exposed to oxygen. More detailed studies on the interactions between the microbial communities of seagrass rhizospheres and plant activity are, however, required to elucidate these aspects.

The present study documents the complementary potential of planar optodes for studies on rhizosomal  $O_2$  dynamics. More work is required to evaluate the quantitative effects of placing a wall along the roots, but the ability to resolve real-time spatial and temporal dynamics is apparent. As the environmental controls (i.e., bed ventilation, light availability, etc.) are highly variable in situ, it is to be expected that the in situ ROL express extreme dynamics. An inverted periscope obtaining benthic in situ  $O_2$  images has been developed (Glud et al. 2001) and has been used for studying macrofaunal activity and spatial variability in benthic  $O_2$  distribution (Wenzhöfer and Glud 2004; Glud et al. 2005). Work in natural seagrass beds is foreseen.

## References

- ARMSTRONG, W. 1971. Radial oxygen losses from intact rice roots as affected by distance from the apex, respiration and waterlogging. *Physiol. Plant.* **25**: 192–197.
- , D. COUSINS, J. ARMSTRONG, D. W. TURNER, AND P. M. BECKETT. 2000. Oxygen distribution in wetland plant roots and permeability barriers to gas-exchange with the rhizosphere: A microelectrode and modelling study with *Phragmites australis*. *Ann. Bot.* **86**: 687–703.
- BARNABAS, A. D. 1994a. Apoplastic and symplastic pathways in leaves and roots of the seagrass *Halodule uninervis* (Forssk) Aschersp. *Aquat. Bot.* **47**: 155–174.
- . 1994b. Anatomical, histochemical and ultrastructural features of the seagrass *Phyllospadix scouleri* Hook. *Aquat. Bot.* **49**: 167–182.
- . 1996. Casparian band-like structures in the root hypodermis of some aquatic angiosperms. *Aquat. Bot.* **55**: 217–225.
- BLAABJERG, V., K. N. MOURITSEN, AND K. FINSTER. 1998. Diel

- cycles of sulphate reduction rates in sediments of a *Zostera marina* bed (Denmark). *Aquat. Microb. Ecol.* **15**: 97–102.
- BORUM, J., O. PEDERSEN, T. M. GREVE, T. A. FRANKOVICH, J. C. ZIEMAN, J. W. FOURQUREAN, AND C. J. MADDEN. 2005. The potential role of plant oxygen and sulphide dynamics in die-off events of the tropical seagrass, *Thalassia testudinum*. *J. Ecol.* **93**: 148–158.
- , K. SAND-JENSEN, T. BINZER, O. PEDERSEN, AND T. M. GREVE. In press. Oxygen movement in seagrasses. In E. W. D. Larkum, R. J. Orth, and C. M. Duarte [eds.], *Seagrasses: Biology, ecology and their conservation*. Springer.
- CAFFREY, J. M. AND W. M. KEMP. 1991. Seasonal and spatial patterns of oxygen production, respiration and root rhizome release in *Potamogeton perfoliatus* L. and *Zostera marina* L. *Aquat. Bot.* **40**: 109–128.
- CHARPY-ROUBAUD, C., AND A. SOURNIA. 1990. The comparative estimation of phytoplanktonic and microphytobenthic production in the oceans. *Mar. Microb. Food Webs* **4**: 31–57.
- COLMER, T. D. 2003. Long-distance transport of gases in plants: A perspective on internal aeration and radial oxygen loss from roots. *Plant Cell Environ.* **26**: 17–36.
- CONNELL, E. L., T. D. COLMER, AND D. I. WALKER. 1999. Radial oxygen loss from intact roots of *Halophila ovalis* as a function of distance behind the root tip and shoot illumination. *Aquat. Bot.* **63**: 219–228.
- DE BEER, D., AND OTHERS. 2005. Transport and mineralization rates in North Sea sandy intertidal sediments, Sylt-Romo Basin, Wadden Sea. *Limnol. Oceanogr.* **50**: 113–127.
- FENCHEL, T. 1996. Worm burrows and oxic microniches in marine sediment. 1. Spatial and temporal scales. *Mar. Biol.* **127**: 289–295.
- GLUD, R. N., J. K. GUNDERSEN, H. ROY, AND B. B. JØRGENSEN. 2003. Seasonal dynamics of benthic O<sub>2</sub> uptake in a semi-enclosed bay: Importance of diffusion and faunal activity. *Limnol. Oceanogr.* **48**: 1265–1276.
- , N. B. RAMSING, J. K. GUNDERSEN, AND I. KLIMANT. 1996. Planar optodes: A new tool for fine scale measurements of two-dimensional O<sub>2</sub> distribution in benthic communities. *Mar. Ecol. Prog. Ser.* **140**: 217–226.
- , A. TENGBERG, M. KÜHL, P. O. J. HALL, I. KLIMANT, AND G. HOST. 2001. An in situ instrument for planar O<sub>2</sub> optode measurements at benthic interfaces. *Limnol. Oceanogr.* **46**: 2073–2080.
- , F. WENZHÖFER, A. TENGBERG, M. MIDDELBOE, K. OGURI, AND H. KITAZATO. 2005. Benthic oxygen distribution in central Sagami Bay, Japan: In situ measurements by microelectrodes and planar optodes. *Deep-Sea Res.* **52**: 1974–1987.
- GREVE, T. M., J. BORUM, AND O. PEDERSEN. 2003. Meristematic oxygen variability in eelgrass (*Zostera marina*). *Limnol. Oceanogr.* **48**: 210–216.
- GUNDERSEN, J. K., N. B. RAMSING, AND R. N. GLUD. 1998. Predicting the signal of O<sub>2</sub> microsensors from physical dimensions, temperature, salinity, and O<sub>2</sub> concentration. *Limnol. Oceanogr.* **43**: 1932–1937.
- HOLMER, M., AND E. J. BONDGAARD. 2001. Photosynthetic and growth response of eelgrass to low oxygen and high sulfide concentrations during hypoxic events. *Aquat. Bot.* **70**: 29–38.
- , B. GRIBSHOLT, AND E. KRISTENSEN. 2002. Effects of sea level rise on growth of *Spartina anglica* and oxygen dynamics in rhizosphere and salt marsh sediments. *Mar. Ecol. Prog. Ser.* **225**: 197–204.
- , AND S. L. NIELSEN. 1997. Sediment sulfur dynamics related to biomass-density patterns in *Zostera marina* (eelgrass) beds. *Mar. Ecol. Prog. Ser.* **146**: 163–171.
- HOLST, G., AND B. GRUNWALD. 2001. Luminescence lifetime imaging with transparent oxygen optodes. *Sensors Actuators B* **74**: 78–90.
- , O. KOHLS, I. KLIMANT, B. KÖNIG, M. KÜHL, AND T. RICHTER. 1998. A modular luminescence lifetime imaging system for mapping oxygen distribution in biological samples. *Sensors Actuators B* **51**: 163–170.
- ISAKSEN, M. F., AND K. FINSTER. 1996. Sulphate reduction in the root zone of the seagrass *Zostera noltii* on the intertidal flats of a coastal lagoon (Arcachon, France). *Mar. Ecol. Prog. Ser.* **137**: 187–194.
- JENSEN, S. I., M. KÜHL, R. N. GLUD, L. B. JØRGENSEN, AND A. PRIEMÉ. 2005. Oxic microzones and radial oxygen loss from roots of *Zostera marina*. *Mar. Ecol. Prog. Ser.* **293**: 49–58.
- JØRGENSEN, B. B., AND N. P. REVSBECH. 1985. Diffusive boundary-layers and the oxygen-uptake of sediments and detritus. *Limnol. Oceanogr.* **30**: 111–122.
- LARKUM, A. W. D., G. ROBERTS, J. KUO, AND S. STROTHER. 1989. Gaseous movements in seagrasses, p. 686–722. In A. W. D. Larkum, A. J. McComb, and S. A. Shepherd [eds.], *Biology of seagrasses*. Elsevier.
- MCDONALD, M. P., N. W. GALWEY, AND T. D. COLMER. 2001. Waterlogging tolerance in the tribe Triticeae: The adventitious roots of *Critesion marinum* have a relatively high porosity and a barrier to radial oxygen loss. *Plant Cell Environ.* **24**: 585–596.
- MEILE, C., AND P. VAN CAPPELLEN. 2003. Global estimates of enhanced solute transport in marine sediments. *Limnol. Oceanogr.* **48**: 777–786.
- MORIARTY, D. J. W., R. L. IVERSON, AND P. C. POLLARD. 1986. Exudation of organic-carbon by the seagrass *Halodule wrightii* Aschers and its effect on bacterial growth in the sediment. *J. Exp. Mar. Biol. Ecol.* **96**: 115–126.
- OLESEN, B., AND K. SAND-JENSEN. 1994. Biomass-density patterns in the temperate seagrass *Zostera-marina*. *Mar. Ecol. Prog. Ser.* **109**: 283–291.
- PEDERSEN, O., T. BINZER, AND J. BORUM. 2004. Sulphide intrusion in eelgrass (*Zostera marina* L.). *Plant Cell Environ.* **27**: 595–602.
- , J. BORUM, C. M. DUARTE, AND M. D. FORTES. 1998. Oxygen dynamics in the rhizosphere of *Cymodocea rotundata*. *Mar. Ecol. Prog. Ser.* **169**: 283–288.
- , ———, ———, AND ———. 1999. Oxygen dynamics in the rhizosphere of *Cymodocea rotundata* (vol. 169, p. 283, 1998). *Mar. Ecol. Prog. Ser.* **178**: 310.
- PENHALE, P. A., AND R. G. WETZEL. 1983. Structural and functional adaptations of eelgrass (*Zostera marina* L.) to the anaerobic sediment environment. *Can. J. Bot.* **61**: 1421–1428.
- POLLARD, P. C., AND D. J. W. MORIARTY. 1991. Organic-carbon decomposition, primary and bacterial productivity, and sulfate reduction, in tropical seagrass beds of the Gulf of Carpentaria, Australia. *Mar. Ecol. Prog. Ser.* **69**: 149–159.
- PRECHT, E., U. FRANKE, L. POLERECKY, AND M. HUETTEL. 2004. Oxygen dynamics in permeable sediments with wave-driven pore water exchange. *Limnol. Oceanogr.* **49**: 693–705.
- REVSBECH, N. P. 1989. An oxygen microsensor with a guard cathode. *Limnol. Oceanogr.* **34**: 474–478.
- RISGAARD-PETERSEN, N., T. DALSGAARD, S. RYSGAARD, P. B. CHRISTENSEN, J. BORUM, K. MCGLATHERY, AND L. P. NIELSEN. 1998. Nitrogen balance of a temperate eelgrass *Zostera marina* bed. *Mar. Ecol. Prog. Ser.* **174**: 281–291.
- SAND-JENSEN, K., C. PRAHL, AND H. STOKHOLM. 1982. Oxygen release from roots of submerged aquatic macrophytes. *Oikos* **38**: 349–354.
- SORRELL, B. K., AND W. ARMSTRONG. 1994. On the difficulties of measuring oxygen release by root systems of wetland plants. *J. Ecol.* **82**: 177–183.

- , AND P. I. BOON. 1994. Convective gas-flow in *Eleocharis-sphacelata* R. Br.: Methane transport and release from wetlands. *Aquat. Bot.* **47**: 197–212.
- VERHAGEN, F. J. M., P. E. J. HAGEMAN, J. W. WOLDENDORP, AND H. J. LAANBROEK. 1994. Competition for ammonium between nitrifying bacteria and plant-roots in soil in pots—effects of grazing by flagellates and fertilization. *Soil Biol. Biochem.* **26**: 89–96.
- WENZHÖFER, F., AND R. N. GLUD. 2004. Small-scale spatial and temporal variability in coastal benthic O<sub>2</sub> dynamics: Effects of fauna activity. *Limnol. Oceanogr.* **49**: 1471–1481.

*Received: 6 June 2005*  
*Accepted: 20 October 2005*  
*Amended: 16 November 2005*